AD-A064 676 AIR FORCE ARMAMENT LAB EGLIN AFB FLA F/G 13/13
FAILURE AND POST BUCKLING BEHAVIOR OF THIN CYLINDRICAL SHELLS.(U)
APR 77 W S STRICKLAND, C A ROSS

UNCLASSIFIED AFATL-TR-77-52 NL

1 OF 1
AD
A064676

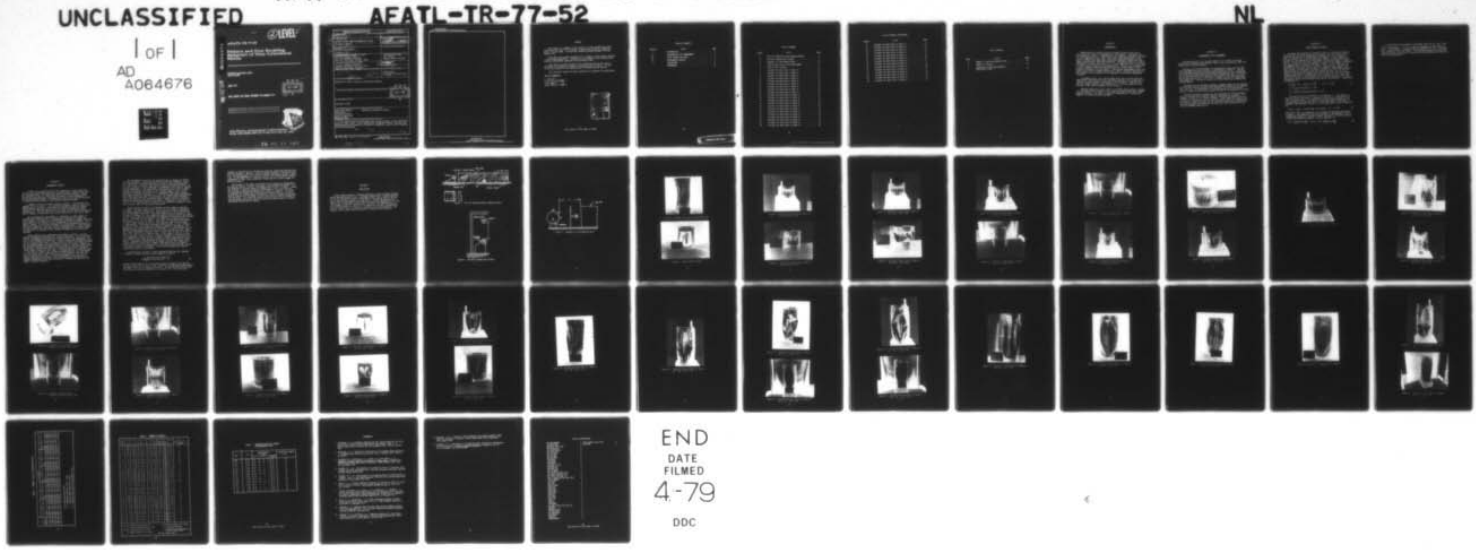

END
DATE
FILMED
4-79
DDC

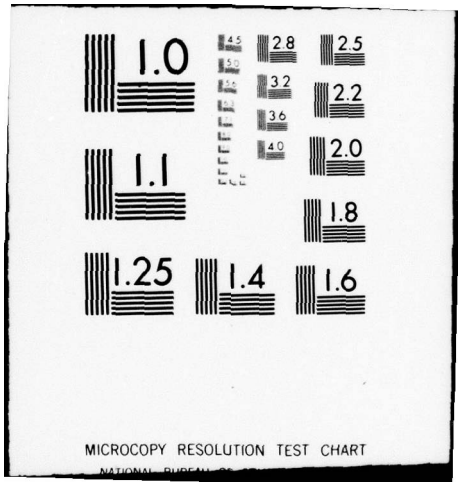
1.0
1.1
1.25
1.4
1.6
1.8
2.0
2.2
2.5
2.8
3.2
3.6
4.0
MICROCOPY RESOLUTION TEST CHART

(2) LEVEL II

AFATL-TR-77-52

Failure and Post Buckling Behavior of Thin Cylindrical Shells

VULNERABILITY ASSESSMENTS BRANCH
ANALYSIS DIVISION

APRIL 1977

FINAL REPORT FOR PERIOD NOVEMBER 1975-JANUARY 1977

Approved for public release; distribution unlimited

Air Force Armament Laboratory
AIR FORCE SYSTEMS COMMAND ★ UNITED STATES AIR FORCE ★ EGLIN AIR FORCE BASE, FLORIDA

SECURITY CLASSIFICATION OF THIS PAGE (When Data Entered)

REPORT DOCUMENTATION PAGE

READ INSTRUCTIONS BEFORE COMPLETING FORM

1. REPORT NUMBER: AFATL-TR-77-52
2. GOVT ACCESSION NO.
3. RECIPIENT'S CATALOG NUMBER

4. TITLE (and Subtitle): FAILURE AND POST BUCKLING BEHAVIOR OF THIN CYLINDRICAL SHELLS.

5. TYPE OF REPORT & PERIOD COVERED: Final Report. November 1975 — January 1977

6. PERFORMING ORG. REPORT NUMBER

7. AUTHOR(s): William S. Strickland; Claudius A. Ross

8. CONTRACT OR GRANT NUMBER(s)

9. PERFORMING ORGANIZATION NAME AND ADDRESS: Analysis Division (DLYV), Air Force Armament Laboratory, Eglin Air Force Base, Florida 32542

10. PROGRAM ELEMENT, PROJECT, TASK AREA & WORK UNIT NUMBERS: JON 25490214; Program Element 62602F

11. CONTROLLING OFFICE NAME AND ADDRESS: Air Force Armament Laboratory, Armament Development and Test Center, Eglin Air Force Base, Florida

12. REPORT DATE: April 1977

13. NUMBER OF PAGES: 47

14. MONITORING AGENCY NAME & ADDRESS (if different from Controlling Office)

15. SECURITY CLASS. (of this report): UNCLASSIFIED

15a. DECLASSIFICATION/DOWNGRADING SCHEDULE

16. DISTRIBUTION STATEMENT (of this Report)

Approved for public release; distribution unlimited.

17. DISTRIBUTION STATEMENT (of the abstract entered in Block 20, if different from Report)

18. SUPPLEMENTARY NOTES

Available in DDC.

19. KEY WORDS (Continue on reverse side if necessary and identify by block number)

Impulsive Loadings
Blast Loads
Cylindrical Shells
Fuel Air Explosives
Buckling Modes
Loading on Cylindrical Surface

20. ABSTRACT (Continue on reverse side if necessary and identify by block number)

This report presents experimental data on the response of thin cylindrical shells to blast loads. Blast loading over cylindrical surfaces, failure, and buckling modes are examined in an effort to establish a base for post buckling and failure modelings.

DD FORM 1 JAN 73 1473 EDITION OF 1 NOV 65 IS OBSOLETE

UNCLASSIFIED

SECURITY CLASSIFICATION OF THIS PAGE (When Data Entered)

PREFACE

This report is a summary of the results of a test program that established base-line data for the dynamic response and failure of cylindrical shells to blast loads. The work was conducted between November 1975 and January 1977.

This report was jointly prepared by Dr. Claudius A. Ross and Mr. William S. Strickland (AFTAL/DLYV). Personnel of the Terminal Effects Experimental Facility (AFATL/DLDT) supported the experimental work.

This report has been reviewed by the Information Office (OI) and is releasable to the National Technical Information Service (NTIS). At NTIS it will be available to the general public including foreign nations.

This technical report has been reviewed and is approved for publication.

FOR THE COMMANDER

J. R. MURRAY
Chief, Analysis Division

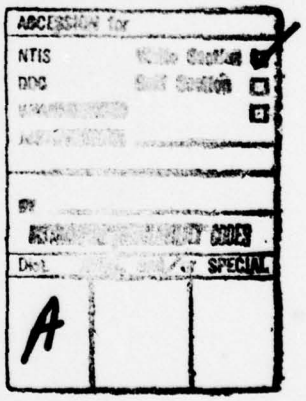

(The reverse of this page is blank)

TABLE OF CONTENTS

LIST OF FIGURES

List of Figures (Continued)

List of Tables

SECTION I

INTRODUCTION

Dynamic plastic response of metal cylindrical shells subjected to sharp edge blast loads is mathematically very complex. The overall plastic deformation process is complicated by the buckling phenomenon associated with the compressive load. Due to the highly complicated nature of the overall response many approximate analytical solutions coupled with experimental observations, have been formulated. The general results of typical approximate solutions (References 1, 2, 3) are expressions for a given level of damage often displayed as iso-damage curves. These curves are generally a plot of impulse versus peak blast pressure for varying values of the geometric parameters of the cylinder. Considerable experimental work using actual blast loads by Schuman (References 4 and 5), Lindberg (Reference 3) and presently by the authors has not completely verified the approximate solutions.

Iso-damage curves, for a given damage level, may be drawn using the experimental observations and the approximate methods, but a prediction of failure for actual material separation is not available. Even the large and more complex computer codes (References 6, 7, 8) are limited in this area due to the lack of adequate failure criteria.

The main objective of this study is to further define plastic response of cylindrical shells exposed to mild transverse blast loads which produce material rupture. The study is essentially experimental in nature with emphasis on failure and buckling modes.

SECTION II

EXPERIMENTAL TEST ARRANGEMENT

Cylindrical shells of a constant radius of 6.0 inches of varying lengths and thicknesses were tested in both a fuel air explosion (FAE) and high explosive (HE) environment.

Testing in an FAE environment was accomplished using a gas bag technique developed previously and shown schematically in Figure 1. The bag was constructed using polyurethane plastic stretched taut on a galvanized pipe frame and held together with 3M Paklon® transparent tape. A 100-gram disc of green Detasheet and detonator were placed at the end of the bag. The bag was then partially filled with 2 pounds of methyl acetylene propadiene (MAPP) gas. The gas-air mixture was then mixed using a shaded pole electric motor.

Detonation of the Detasheet produces a Chapman-Jouget wave of constant velocity and reflected pressure which impinges on the shell at the opposite end of the bag. The magnitudes of the peak pressure and impulse were varied by adjusting the distance between the end of the bag and the cylinder.

Testing of several cylinders was also completed in an HE environment using 13.75-pound 50/50 Pentolite spheres hung above the cylinder. A schematic of this test is shown in Figure 2. The charge radius (D/A) was varied to give peak pressures and specific impulse similiar to that of the FAE output. Calibration shots of the spherical devices were accomplished and good agreement was found with the analytical and experimental values given by Goodman (Reference 9).

SECTION III

BLAST LOADING ON SHELLS

To analyze the response of cylindrical shells to blast, the load distribution over the shell surface must be known. For the purpose of this study the distribution was determined experimentally, and is reported here for possible use in future analytical studies. A thick walled steel cylinder was instrumented at its mid length with PCB piezoelectric transducers. A series of tests were conducted, using the bag setup, to determine the loading from the fuel air explosive. Figure 3 is a schematic of the instrumented shell, and Table 1 is summary of the results. The data are presented for one-quarter of the shell, as symmetry is maintained. The data in Table 1 are accurate to within 15 percent or better, and represents loading estimates on shells inside and outside the bag. Data for a "D" value of zero represent loading on the shells inside the gas bag from the Chapman-Jouget wave. All other data, for D values, of 3 to 6 feet, represent loads from an air shock generated from the bag explosion. The peak pressure was curve fitted from this data and the distribution is represented by Equation (1).

$$P_m = \left[P_s + (P_r - P_s)(\cos\theta)^{1.8}\right] \qquad 0^\circ \leq \theta \leq 90^\circ \qquad (1)$$

P_s = side-on pressure ($\theta = 90^\circ$)

P_r = normal reflected pressure ($\theta = 0^\circ$)

The peak pressure distribution for 90 degrees < θ < 180 degrees, or the back side of the shell, is estimated to be close to constant at the side-on pressure value. The complexity of actual shock interaction and vortex formations on the back side is beyond the scope of this work. A resonable time dependent estimate for the loading may be given by Equation (2).

$$P(\theta,t) = P_m\left[1 - t/\tau(\theta)\right] \exp\left[-\alpha(\theta)t/\tau(\theta)\right] \ldots . 0^\circ < \theta < 90^\circ \qquad (2)$$

Note that α and τ are functions of θ, and must be obtained from the data in Table 1. An estimate for the decay constant is determined by first integrating Equation (2) between t equals zero and τ, to obtain an expression for the cumulative impulse given as Equation (3).

$$I(\theta) = P_m\left[\tau(\theta)/\alpha(\theta)\right]\left[1 - 1/\alpha(\theta) + \left(1/\alpha(\theta)\right)\left(\exp(-\alpha(\theta))\right)\right] \qquad (3)$$

By substituting experimentally determined values for P_m and I from Table 1 into Equation (3), $\alpha(\theta)$ may be determined for each value of D and θ. If the shell is inside the fuel air mixture, (D = 0), τ is reasonably constant as seen from Table 1. The load distribution for spherical charges has been investigated by Zumwalt and Naik (Reference 10), and this work was not duplicated.

SECTION IV

EXPERIMENTAL RESULTS

A total of 34 cylindrical shells were subjected to blast loads from fuel air and conventional explosives to observe plastic buckling and failure characteristics. All shells were made of 6061-T6 aluminum. Length was varied in an effort to determine the effects of these parameters on failure and buckling modes. The magnitude of the blast load was controlled to produce material rupture or near rupture whenever possible.

A summary of the test results appears in Table 2. The pressure and impulse, P ($\theta = 0$) and I ($\theta = 0$), are those reflected values as seen by the leading edge of the shell. The normally reflected pressure and impulse values for the explosive sphere tests were taken from Goodman's report (Reference 9). The peak pressures are accurate, but the cumulative impulses may be slightly in error due to the relief conditions on the curved shell.

The circumferential mode number, n, represents the whole number of buckled waves around the shell circumference assuming the cylinder was fully buckled. The number n was determined by counting the number of buckles and dividing by the fraction of the circumference that was buckled. This number, however, is not truly representative of the deformation process, in that only a portion of the shell buckles circumferentially. The percentage of shell deformed was relatively constant and column (11) of Table 2 shows that only 25 to 35 percent of the cylinder circumference was plastically deformed.

Before examining the experimental data points in Table 2, certain general deformation characteristics should be mentioned. For all cylinders tested, a fundamental mode shape was observed in the axial direction; i.e., m=1, for the clamped end conditions. Figure 4 shows this fundamental shape for a 0.071-inch thick shell. Failure in the cylinders was always initiated at the clamped boundary and approximately at the $\theta = 0$ point. Rupture of the material generally propagated from this point in both directions around the cylinder circumference; and the resulting failure surface resembled simple tensile failure in thin sheet. A typical failure is shown in Figure 5. The modes or shape of the cylinders circumferentially, as represented by n, are believed to be functions of the shell geometry, material type, and the applied shock loads. If analytical methods are to be used to predict deformation and failure, the circumferential mode shape must be properly determined as the shell stiffness is strongly influenced by the number of buckles generated.

The circumferential mode is the most difficult to analyze or observe from the experiments. Many buckling formulas have been authored, a majority of which were determined empirically. Most of these were generated for static loads, or radical loads uniformly applied around the shell, and were not applicable for the conditions of transverse blast loads as applied in these experiments. The experimental data gathered here tend to support theories of Greenspon (References 1 and 2) which suggest that a given cylindrical shell may be forced into a fundamental buckling or collapse mode, where n might be considered 3 or less, or a higher buckling mode where n has some large value that is a function of the shell length, thickness, radius, and material type. Greenspon further suggests the use of Reynolds (Reference 11)buckling formula to determine n. Comparison of the data in Table 2 to this formulation is discussed in the following paragraphs, along with observed trends and deformation hypotheses.

The data points in Table 2 are ordered in three groups of constant L/D values. The data points for an L/D of 0.39 are listed for decreasing a/h values, (Figures 6 through 16). These data points show a decrease in n as the thickness increases. This trend continues for L/D values of 0.89 (Figures 17 through 28). This grouping, however, contains three data points, 19, 20, and 22, which did not buckle, but appparently deformed in the collapse pattern. The data for L/D values of 1.89 show five collapse patterns at data points 27, 28, 29, 31, and 33. The shells of this group that buckled all had n values between 10 and 25. This indicates that for L/D values of approximately 1 and larger the higher buckling modes are less dominant. The shells tested in this group are shown in Figures 29 through 40. The appearance of a collapse mode and buckling mode in the same cylinder size is apparent in data points (18, 19), (21, 22), (30, 31), and (32, 33). Each set of data represents cylindrical shells tested with the same L/D, and a/h values but with different applied loads. This suggests that for a given shell size there exists a critical load that determines if buckling occurs or a fundamental collapse pattern is formed. Almroth (Reference 12) calculated such critical loads for small deflections and assumed elastic deformation. Experimental determination of dynamic critical load values would require extensive testing and it appears that peak pressure or impulse alone is not a sufficient description of the load to use as critical values to determine collapse or buckling. To vary both experimentally appears impractical outside a shock tunnel.

The data points in Table 2, which indicated buckling, were compared to Reynold's formula Equation (4) and compiled in Table 3.

$$n \approx \frac{\pi D}{2L}\sqrt{\left[(1.626)\,(L/D)\,(a/h)^{\frac{1}{2}} - 1\right]} \qquad (4)$$

Reynold's approximation for n has been rewritten in terms of L/D and a/h for ease of use, and as seen in Table 3 predicts circumferential mode numbers reasonably close for L/D values less than 1. As the L/D value goes to 1.89 the prediction formula overpredicts by a factor of 2. The use of such

formulas is limited until a satisfactory model for separating buckling from collapse patterns is derived. Since the problem appears to be one of stability, the determination of a critical buckling load appears the most attractive. If the appearance of a buckling pattern can be established, formulas independent of load, such as Reynold's formula may be accurate enough for analysis purposes.

The failure of the shells as defined in this report was considered to be material rupture. Briefly discussed in the preceding paragraphs, this was observed to initiate along the clamped edge at the $\theta = 0$ point. Column (8) of Table 2 indicates fracture or nonfracture of the shell material. The approximate centerpoint deflection is shown in column (7). As would be expected, the longer shells deflected more before failure, but due to lack of control over the degree of fracture, little else may be determined from the data. It is believed, however, that failure could be related to the centerpoint deflection, and for a given shell there exists a critical centerpoint deflection for failure.

SECTION V

CONCLUSIONS

Blast loaded cylinders, deformed plastically, show two types of permanently deformed patterns; i.e., a collapse pattern and a buckled pattern. The pattern ultimately formed is dependent on the load as well as the geometric and material properties of the shell. If buckling patterns are formed, the circumferential mode number established as permanent set in the shell appears relatively insensitive to the load. The deformation at or near failure encompasses only 25 to 30 percent of the shell circumference. Failure, defined here as fracture, occurred at the fixed boundaries, and appears to be a simple tensile failure as a result of axial strain.

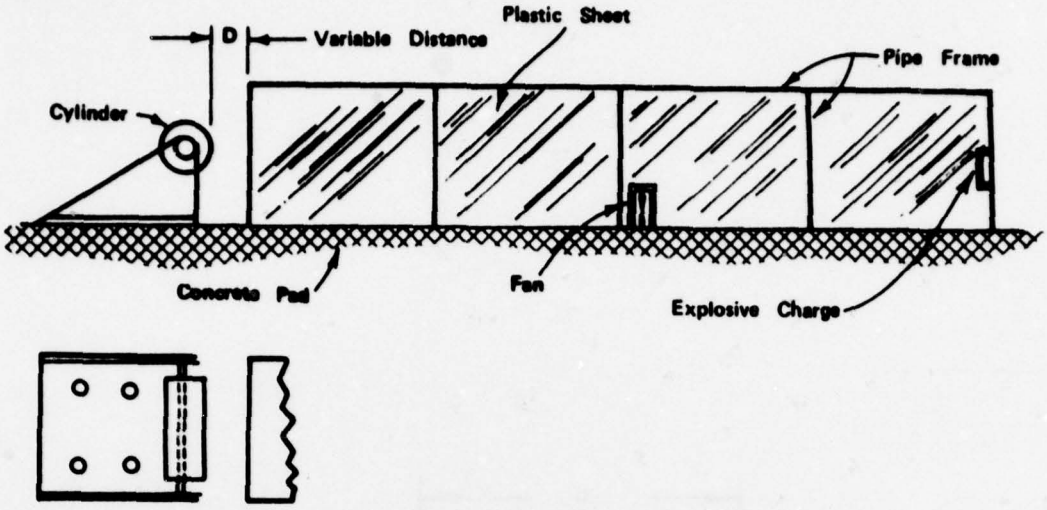

Figure 1. Fuel Air Explosion Blast Loading Fixture

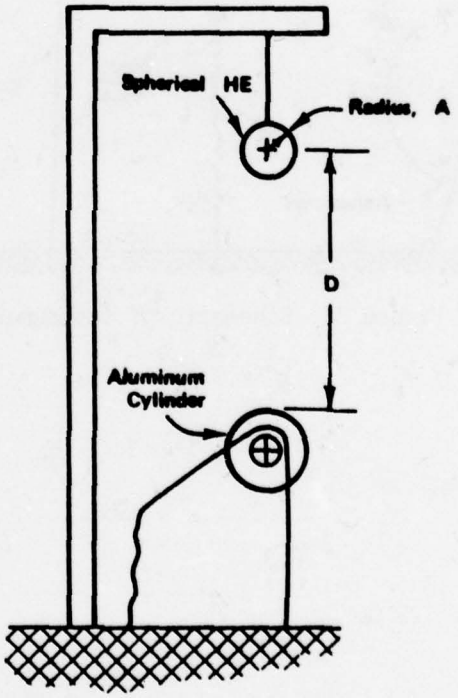

Figure 2. HE Blast Loading Test Fixture

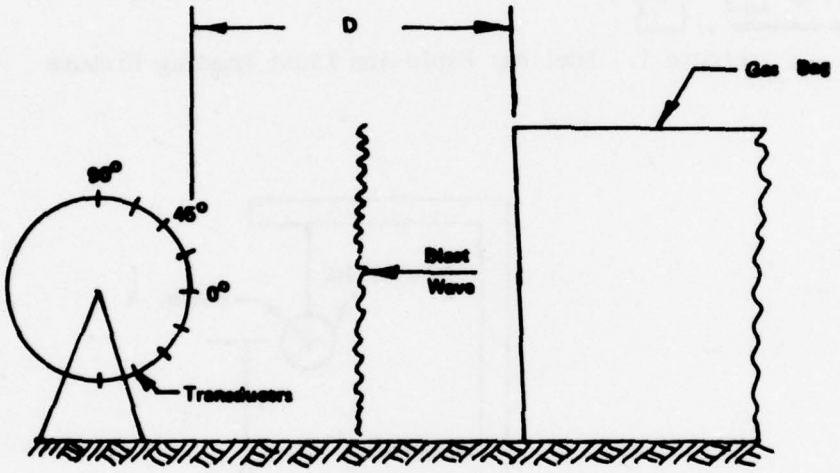

Figure 3. Schematic of Instrumented Shell

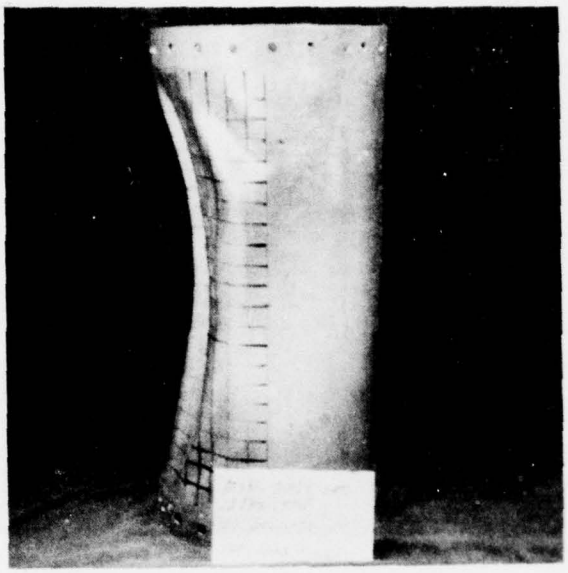

Figure 4. Typical Side View of Axial Mode Shape

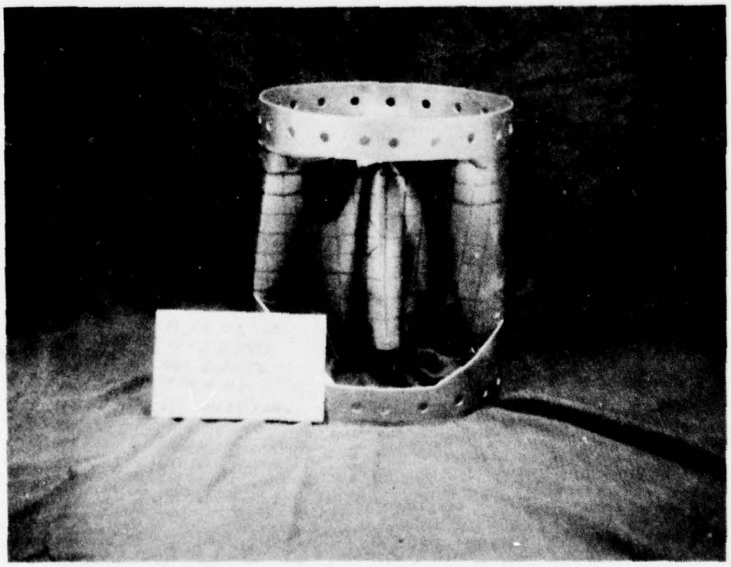

Figure 5. Typical Shell Failure

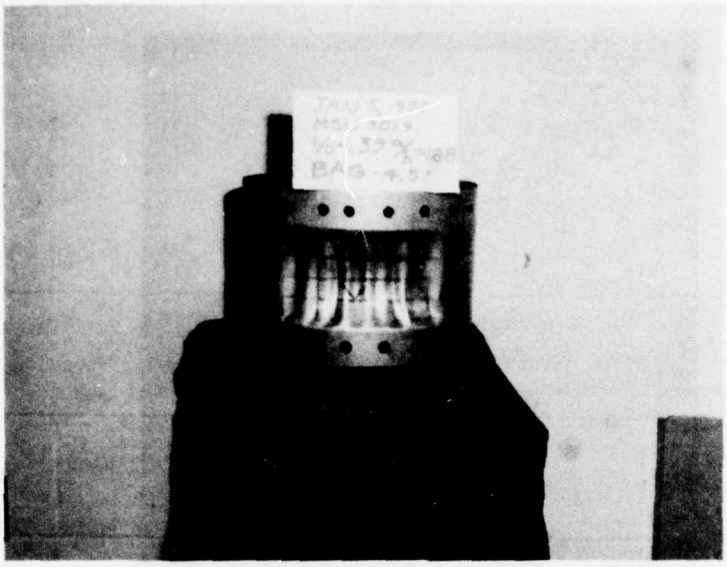

Figure 6. Cylinder for Data Point 1 Table II
a/h = 188 L/D = 0.39

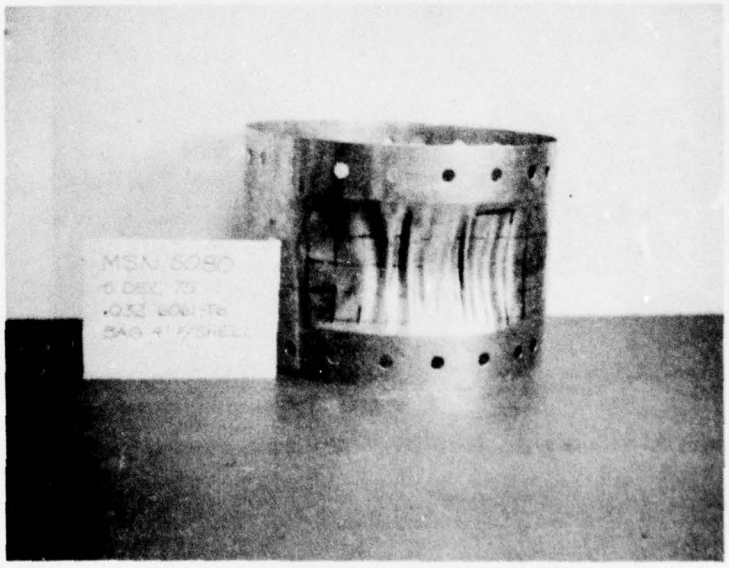

Figure 7. Cylinder for Data Point 2 Table II
a/h = 188 L/D = 0.39

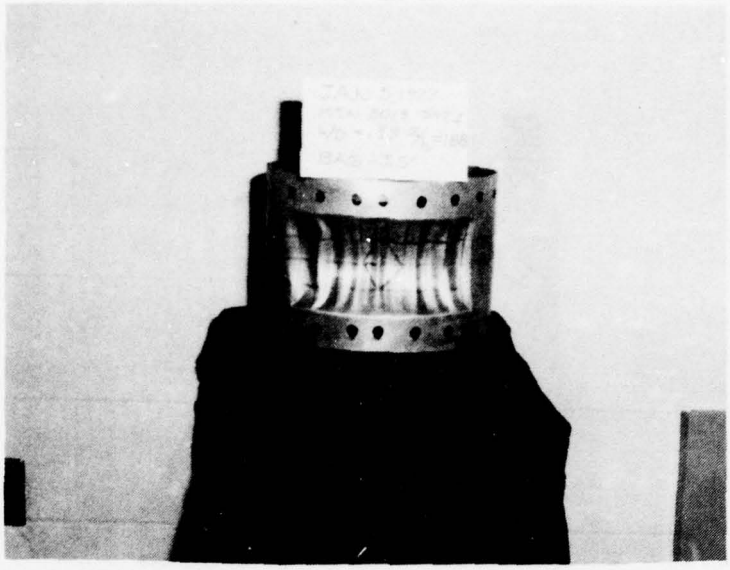

Figure 8. Cylinder for Data Point 3 Table II
a/h = 188 L/D = 0.39

Figure 9. Cylinder for Data Point 4 Table II
a/h = 188 L/D = 0.39

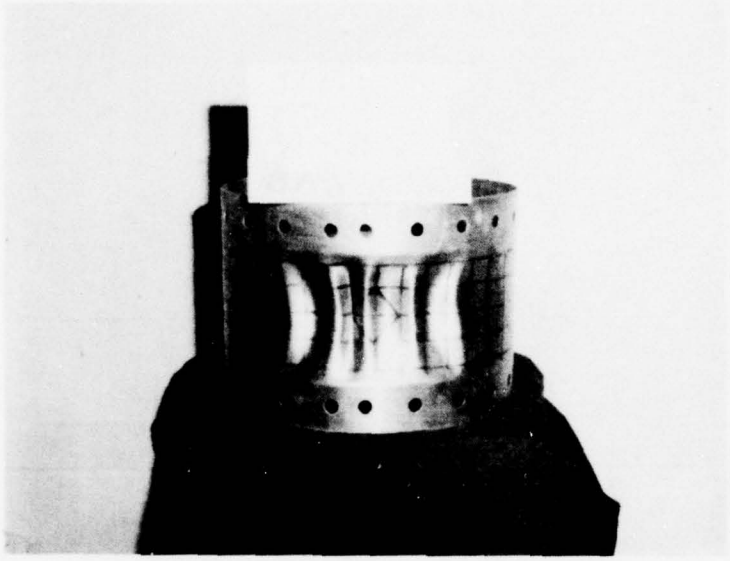

Figure 10. Cylinder for Data Point 5 Table II
a/h = 188 L/D = 0.39

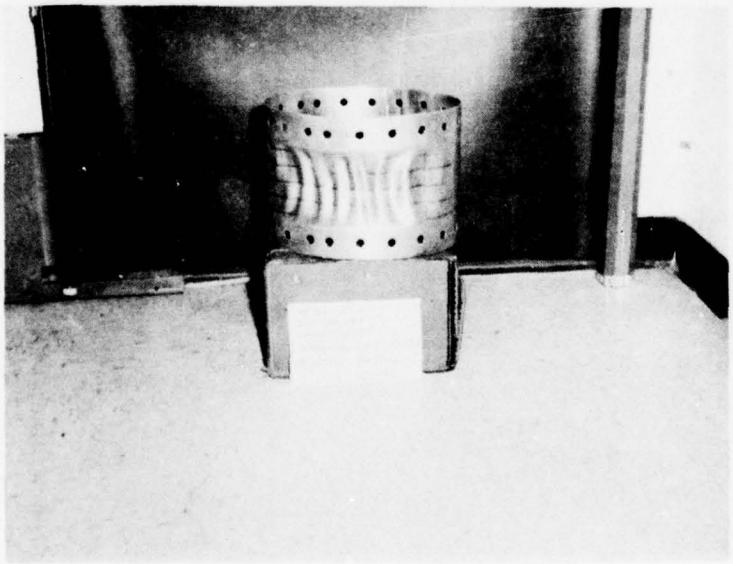

Figure 11. Cylinder for Data Point 6 Table II
a/h = 117 L/D = 0.39

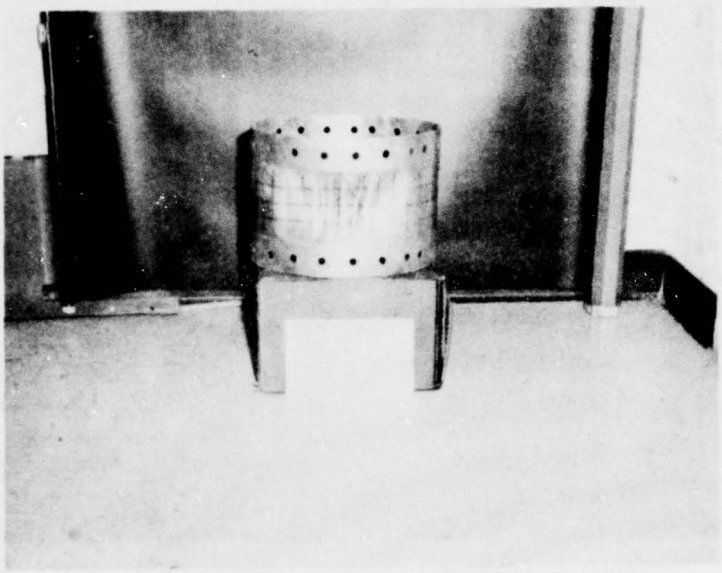

Figure 12. Cylinder for Data Point 7 Table II
a/h = 117 L/D = 0.39

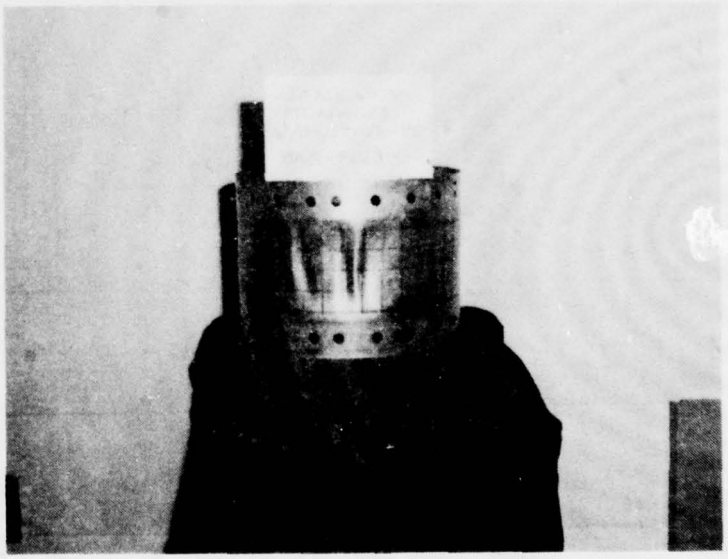

Figure 13. Cylinder for Data Point 8 Table II
a/h = 95 L/D = 0.39

Figure 14. Cylinder for Data Point 9 Table II
a/h = 95 L/D = 0.39

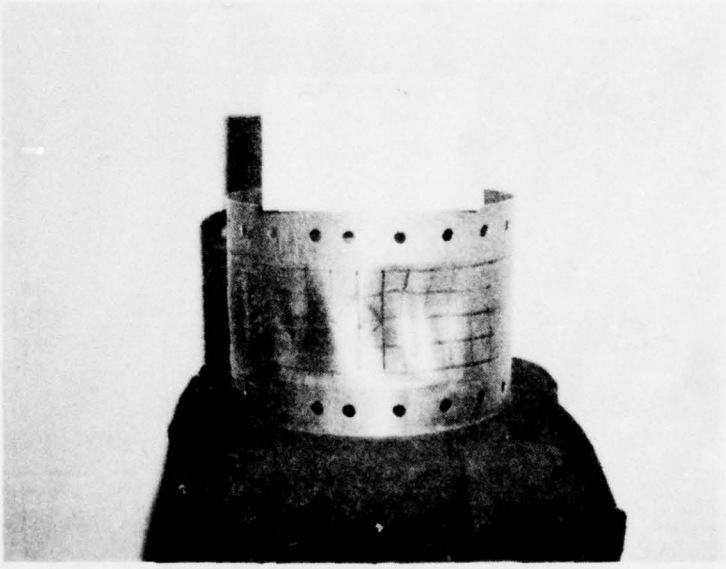

Figure 15. Cylinder for Data Point 10 Table II
a/h = 85 L/D = 0.39

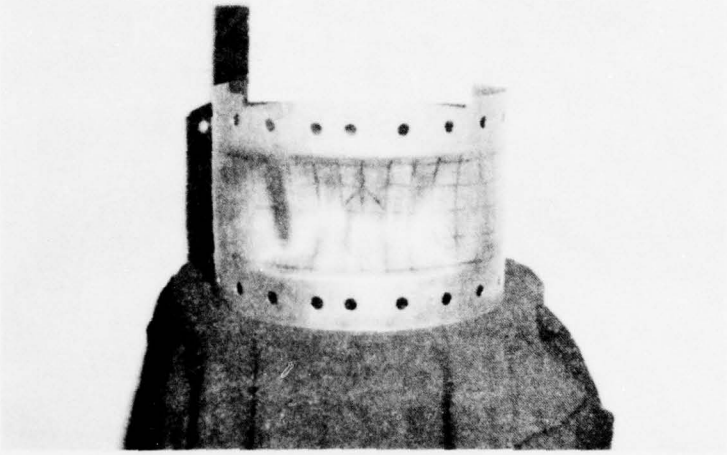

Figure 16. Cylinder for Data Point 11 Table II
a/h = 85 L/D = 0.39

Figure 17. Cylinder for Data Point 12 Table II
a/h = 188 L/D = 0.89

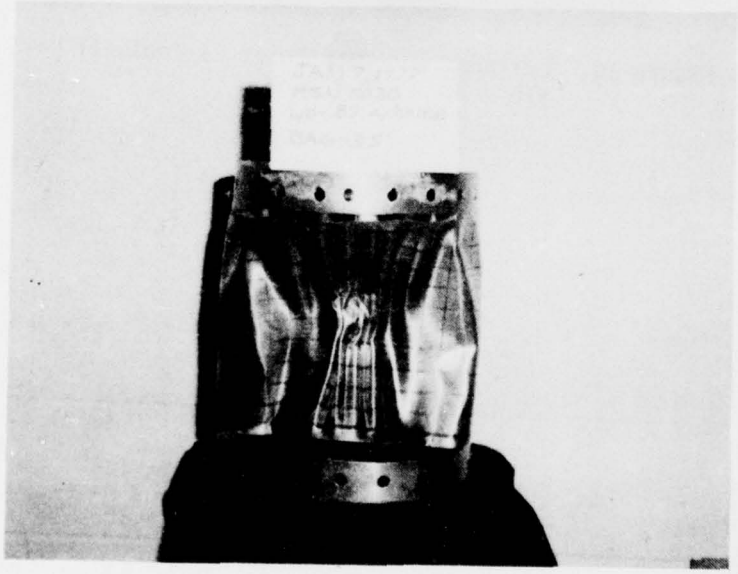

Figure 18. Cylinder for Data Point 13 Table II
a/h = 188 L/D = 0.89

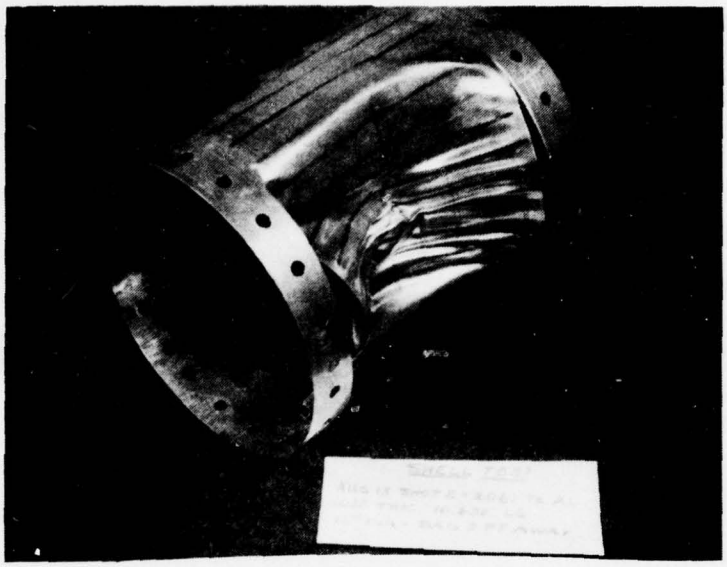

Figure 19. Cylinder for Data Point 14
Table II, a/h = 188 L/D = 0.89

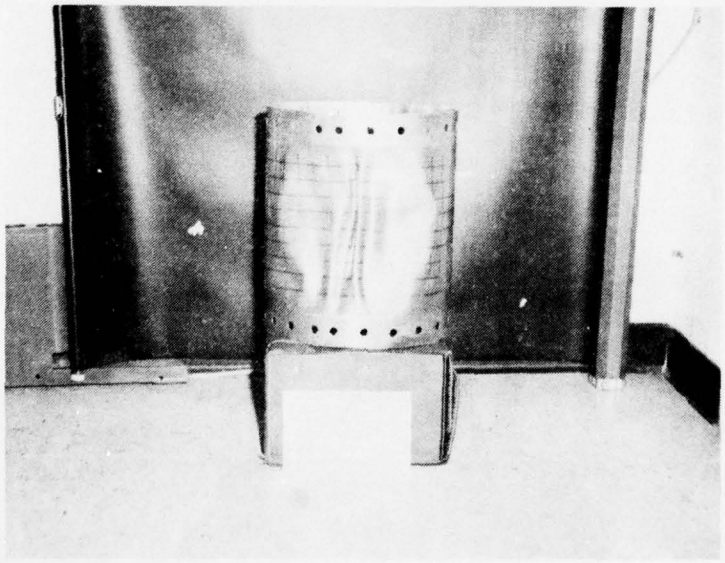

Figure 20. Cylinder for Data Point 15
Table II, a/h = 117 L/D = 0.89

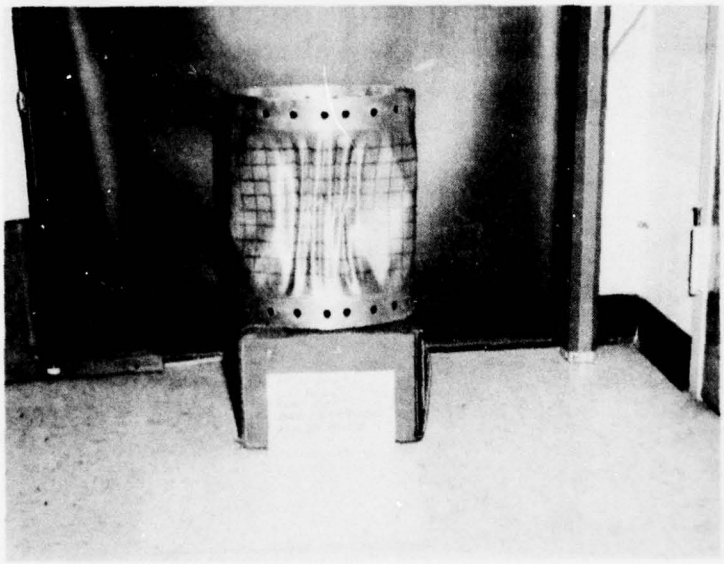

Figure 21. Cylinder for Data Point 16, Table II
a/h = 117 L/D = 0.89

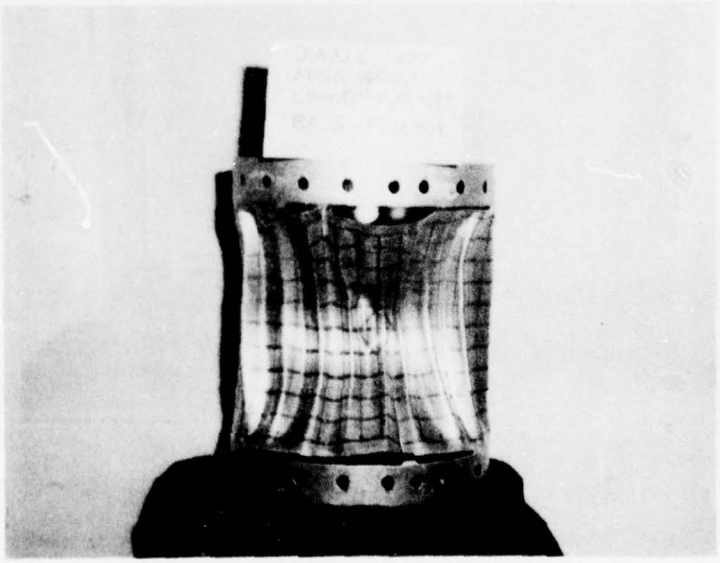

Figure 22. Cylinder for Data Point 17, Table II
a/h = 117 L/D = 0.89

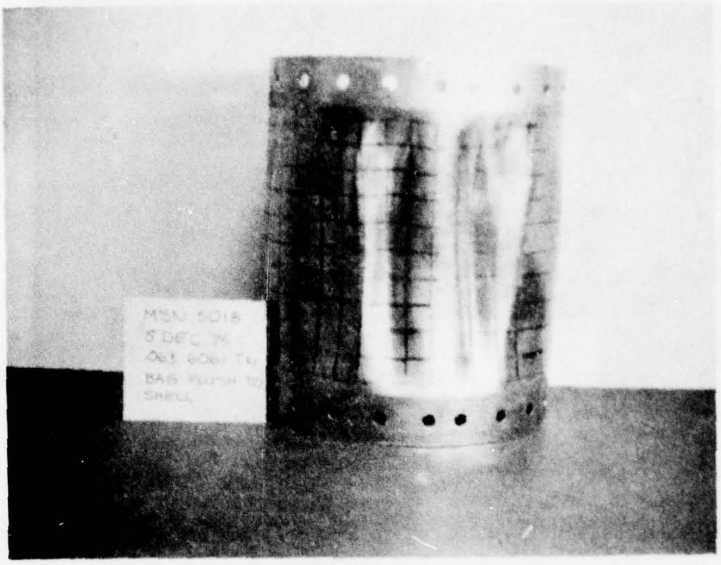

Figure 23. Cylinder for Data Point 18, Table II
a/h = 95 L/D = 0.89

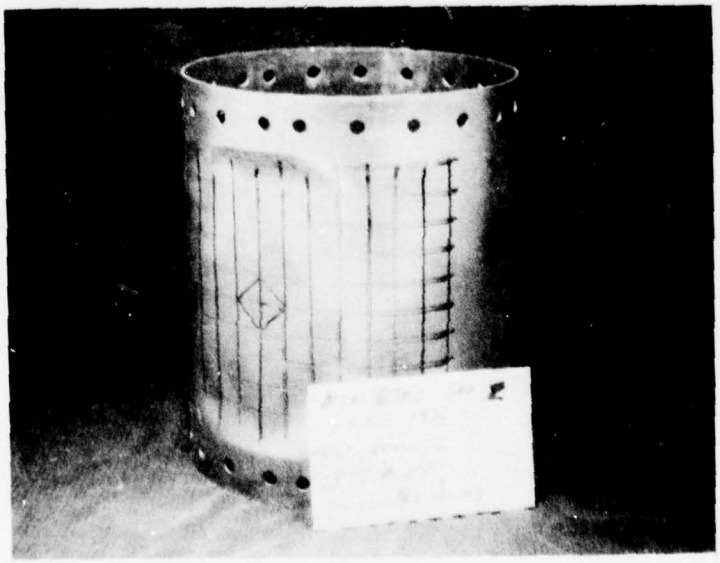

Figure 24. Cylinder for Data Point 19, Table II
a/h = 95 L/D = 0.89

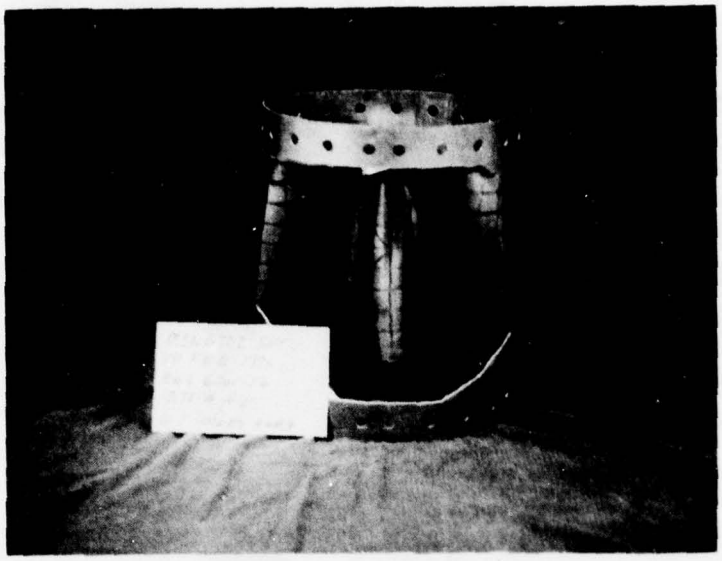

Figure 25. Cylinder for Data Point 20, Table II
a/h = 95 L/D = 0.89

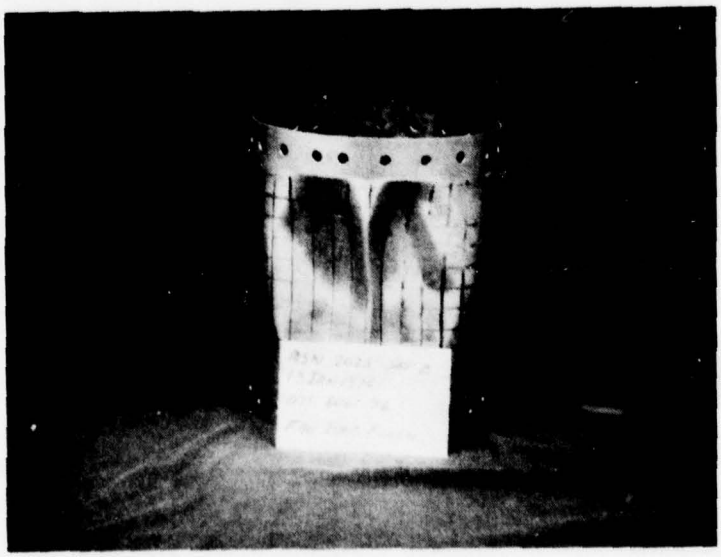

Figure 26. Cylinder for Data Point 21, Table II
a/h = 85 L/D = 0.89

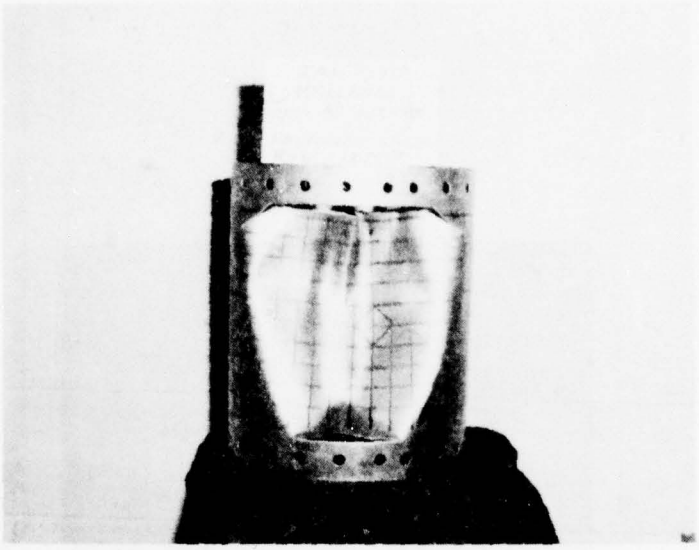

Figure 27. Cylinder for Data Point 22, Table II
a/h = 85 L/D = 0.89

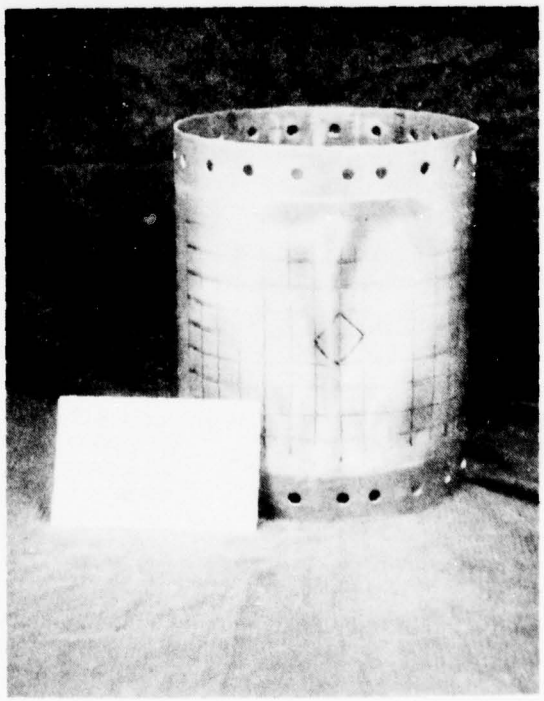

Figure 28. Cylinder for Data Point 23, Table II
a/h = 85 L/D = 0.89

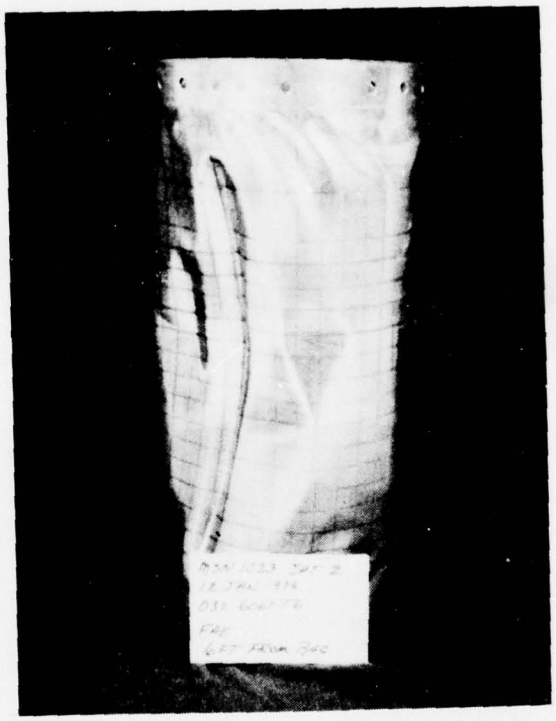

Figure 29. Cylinder for Data Point 24, Table II
a/h = 188 L/D = 1.89

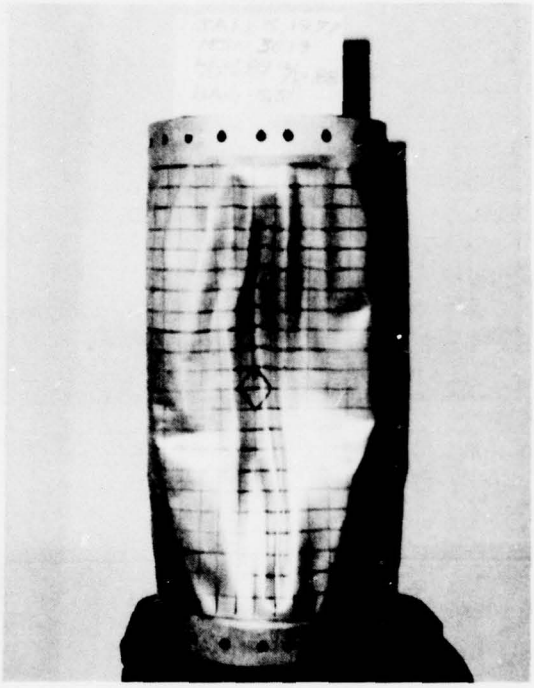

Figure 30. Cylinder for Data Point 25, Table II
a/h = 188 L/D = 1.89

a/h = 188 L/D = 0.39

Figure 31. Cylinder for Data Point 26, Table II
a/h = 188 L/D = 1.89

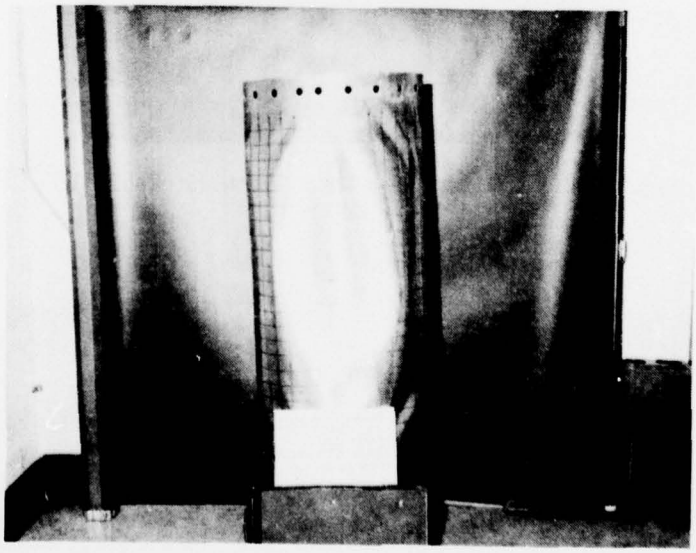

Figure 32. Cylinder for Data Point 27, Table II
a/h = 117 L/D = 1.89

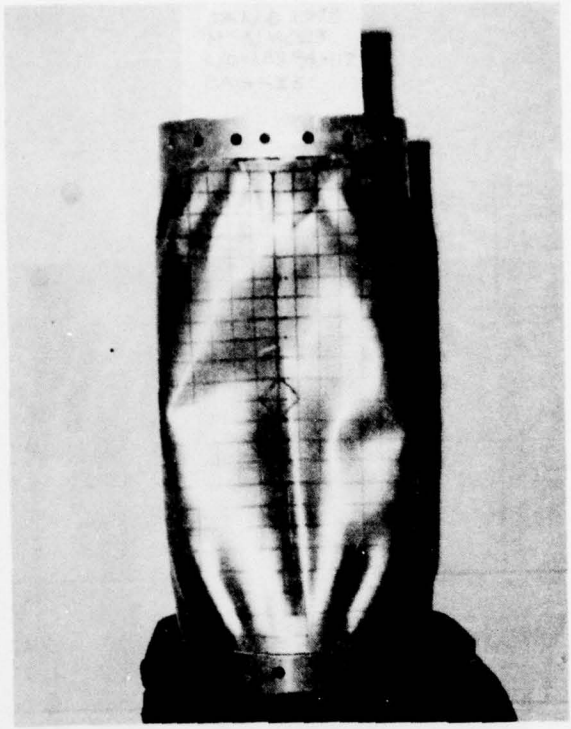

Figure 33. Cylinder for Data Point 28, Table II
a/h = 117, L/D = 1.89

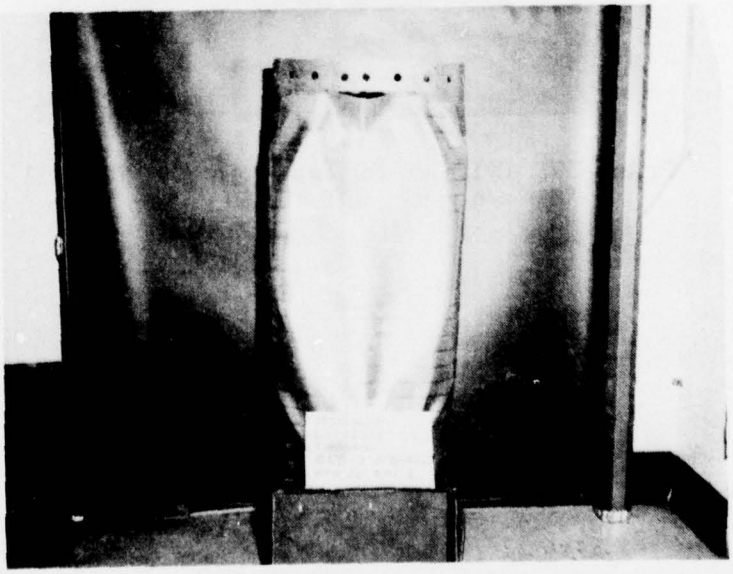

Figure 34. Cylinder for Data Point 29, Table II
a/h = 117 L/D = 1.89

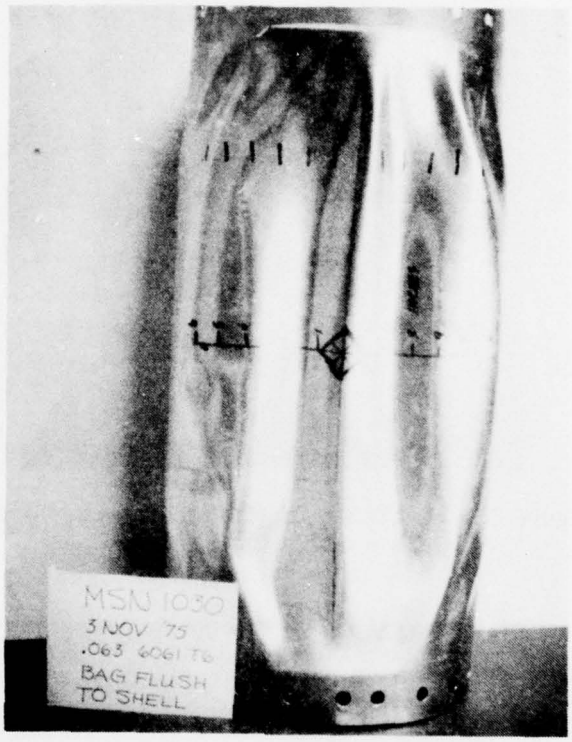

Figure 35. Cylinder for Data Point 30, Table II
a/h = 95 L/D = 1.89

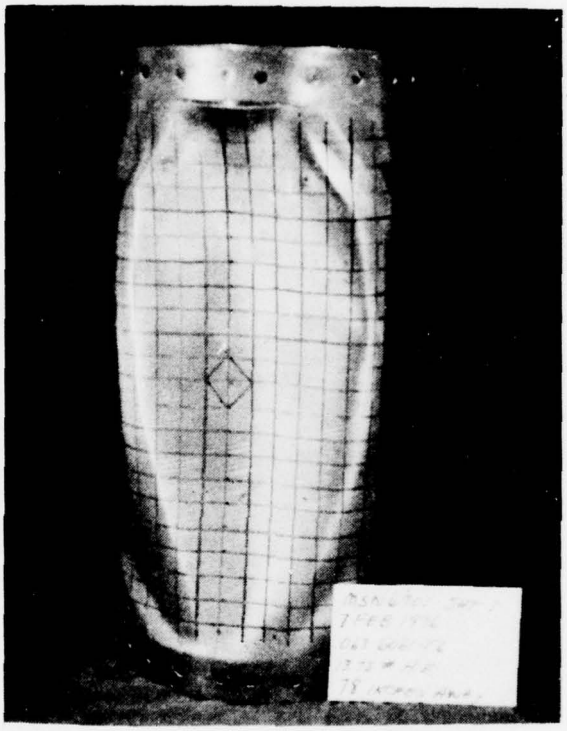

Figure 36. Cylinder for Data Point 31, Table II
a/h = 95 L/D = 1.89

Figure 37. Cylinder for Data Point 32, Table II
a/h = 85 L/D = 1.89

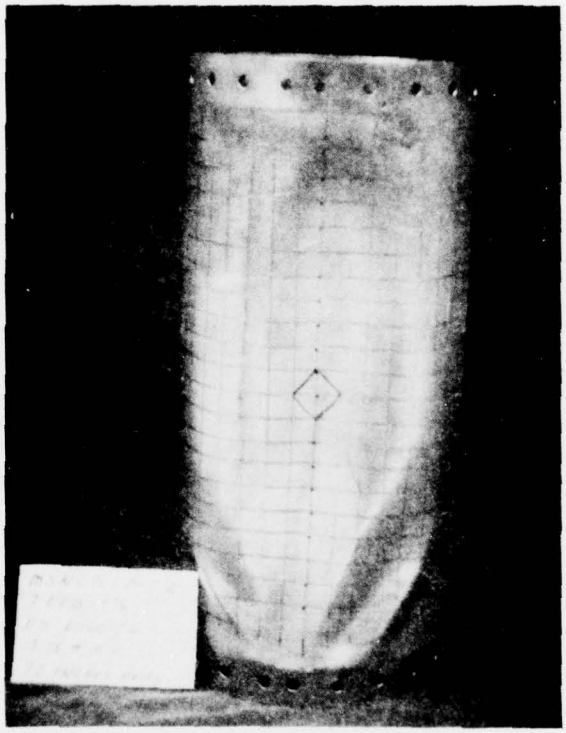

Figure 38. Cylinder for Data Point 33, Table II
a/h = 85 L/D = 1.89

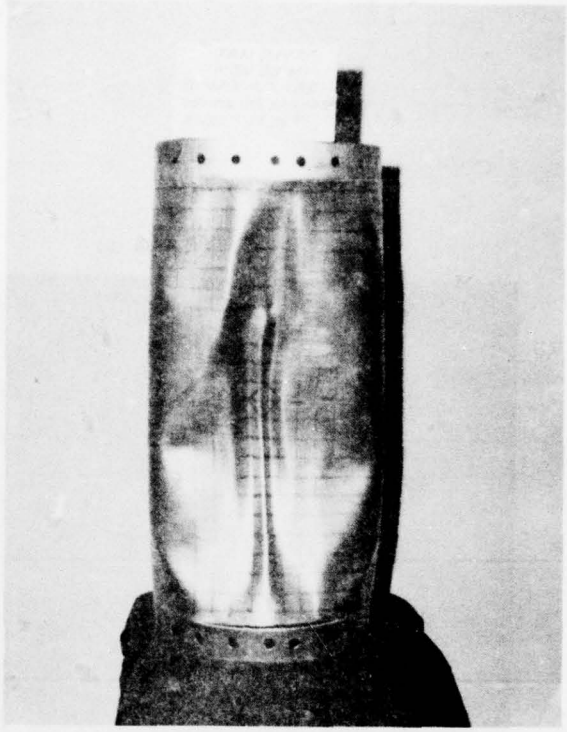

Figure 39. Cylinder for Data Point 34, Table II
a/h = 85 L/D = 1.89

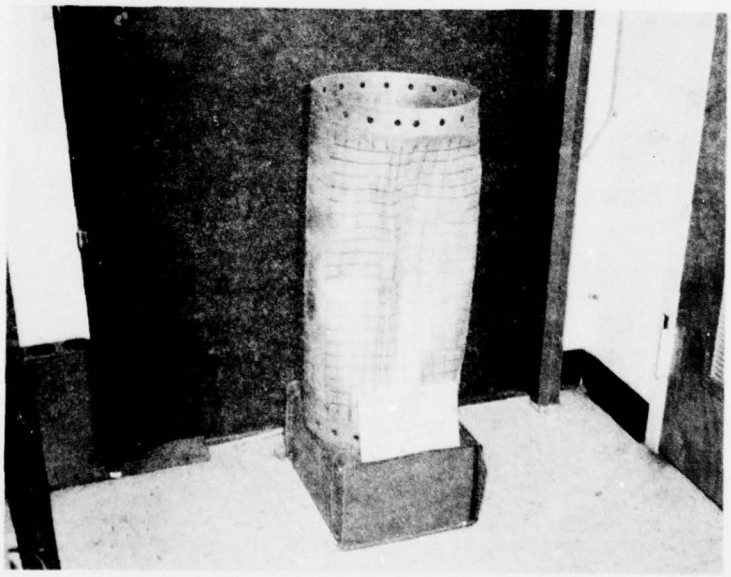

Figure 40. Cylinder for Data Point 35, Table II
a/h = 85 L/D = 1.89

TABLE 1. SUMMARY OF LOAD DISTRIBUTION TESTS

θ in Degrees	D in Feet														
	0			3			4			5			6		
	P_M	I	τ	P_M	I	τ	P_M	I	τ	P_M	I	τ	P_M	I	τ
0	876	105	0.70	706	110	0.84	430	85	0.85	279	67	1.00	203	53	1.40
22.5	810	90	0.68	584	95	0.72	404	80	0.70	260	58	0.94	174	47	0.94
45	630	85	0.67	471	50	0.53	305	40	0.57	177	30	0.75	144	34	0.70
67.5	450	82	0.69	245	30	0.51	155	23	0.55	106	22	0.63	79	16	0.63
90	375	80	0.70	155	10	0.35	95	10	0.35	66	10	0.48	44	7	0.50

P_M = Peak pressure in PSI
I = Cumlative Impulse in PSI - msec
τ = Positive Phase Duration in msec
D = Distance from shell leading edge to bag

TABLE 2. SUMMARY OF RESULTS

(1) Data Point	(2) a/h	(3) L/D	(4) P_M (θ = 0)	(5) I (θ = 0)	(6) n	(7) C.P. Defl.	(8) Material Failure	(9) Load Device	(10) D	(11) Percent of Circum. Deformed
1	188	0.39	350	75	28	0.64	No	Bag	4.5	30
2	188	0.39	430	85	38	0.80	Yes	Bag	4.0	30
3	188	0.39	530	97	34	1.13	Yes	Bag	3.5	—
4	188	0.39	650	110	36	4.10	Yes	Bag	3.0	—
5	117	0.39	650	110	22	0.88	No	Bag	3.0	32
6	117	0.39	875	130	25	0.91	No	Bag	0	34
7	117	0.39	1200	186	30	1.19	No	Pent. Sph.	5.6	25
8	95	0.39	875	130	26	0.40	No	Bag	0	24
9	95	0.39	875	130	26	0.29	No	Bag	0	24
10	85	0.39	2500	280	25	0.54	No	Pent. Sph.	4.1	34
11	85	0.39	3400	338	23	1.04	No	Pent Sph.	3.6	30
12	188	0.89	430	85	32	2.40	Yes	Bag	4.0	34
13	188	0.89	530	97	32	>4.5	Yes	Bag	3.5	—
14	188	0.89	650	110	33	>4.5	Yes	Bag	3.0	—
15	117	0.89	650	110	26	1.56	No	Bag	3.0	32
16	117	0.89	1000	120	34	2.38	Yes	Bag	2.0	36
17	117	0.89	875	130	22	3.25	Yes	Bag	0	—
18	95	0.89	875	130	18	1.20	No	Bag	0	34
19	95	0.89	800	150	3	0.34	No	Pent. Sph.	6.5	24
20	95	0.89	1500	210	3	>4.5	Yes	Pent. Sph.	5.1	—
21	85	0.89	875	130	19	0.95	No	Bag	0	32
22	85	0.89	1000	171	3	3.25	Yes	Pent Sph.	6.0	—
23	85	0.89	1200	186	26	0.63	No	Pent Sph.	5.6	22
24	188	1.89	185	53	13	1.70	Yes	Bag	6.0	34
25	188	1.89	220	58	13	—	No	Bag	5.5	34
26	188	1.89	270	65	19	>4.5	Yes	Bag	5.0	—
27	117	1.89	430	85	3	1.44	No	Bag	4.0	29
28	117	1.89	530	97	3	3.10	Yes	Bag	3.5	—
29	117	1.89	650	110	3	2.88	Yes	Bag	3.0	—
30	95	1.89	875	130	10	2.75	Yes	Bag	0	—
31	95	1.89	800	150	3	2.19	Yes	Pent. Sph	6.5	32
32	85	1.89	875	130	10	2.56	No	Bag	0	37
33	85	1.89	1000	171	3	1.40	No	Pent. Sph.	6.0	32
34	85	1.89	1200	186	25	2.84	Yes	Pent. Sph.	5.6	30
35	85	1.89	1500	210	25	2.78	No	Pent. Sph.	5.1	33

$P_M(\theta = 0)$ = Normally reflected pressure in PSI

$I(\theta = 0)$ = Normally reflected impulse in PSI - msec

C.P. Defl. = Center point deflection in inches

L/D = Length to diameter ratio of cylinder

a/h = Radius to thickness ratio of cylinder

n = Circumferential mode number

0 = distance from shell leading edge to bag or center of pentolite sphere

pent. sph. = pentolite sphere

TABLE 3. COMPARISON BUCKLING FORMULA TO EXPERIMENTAL DATA

a/h	L/D	Experimental n exp.					Reynold's Formula n rey
						Avg.	
188	0.39	28	38	34	36	34	31
117	0.39	22	25	30	—	26	25
95	0.39	26	26	—	—	26	22
85	0.39	25	23	—	—	24	21
188	0.89	32	32	33	—	32	29
117	0.89	26	34	22	—	27	23
95	0.89	18	—	—	—	18	21
85	0.89	19	26	—	—	23	20
188	1.89	13	13	19	—	15	27
117	1.89	—	—	—	—	—	22
95	1.89	10	—	—	—	10	20
85	1.89	10	25	25	—	20	19

(The reverse of this page is blank)

REFERENCES

1. Greenspon, J. E., Collapse, Buckling and Post Failure Behavior of Cylindrical Shells Under Elevated Temperature and Dynamic Loads, J. G. Engineering Research Association, TR-6 November 1956. DDC No. AD 630-269.

2. Greenspon, J. E., Theoretical Calculation of Iso-Damage Characteristics, J. G. Engineering Research Association, TR-10, February 1970. DDC No. AD 869093.

3. Lindberg, H. E. Anderson, D. L., Firth, R. D. and Parker, L. V., Response of Reentry Vehicle-Type Shells to Blast Loads, Standford Research Institution Menlo Park, California. USAF Contract AF04 (694)-655 September 1965.

4. Schuman, W. J. Jr., The Response of Cylindrical Shells to External Blast Loading, BRL Memo Department 1461, Ballistic Research Laboratory Aberdeen Proving Ground, March 1963.

5. Schuman, W. J. Jr., The Response of Cylindrical Shells to External Blast Loading - Part II, BRL Memo Department 1560 Ballistic Research Laboratory Aberdeen Proving Ground, May 1964.

6. Mente, L. J., "Dynamic Nonlinear Response of Cylindrical Shells to Asymmetric Pressure Loading" AIAA Journal, Volume 11, No. 6, June 1973, pp. 793-800.

7. Atluri, S. Witmer, E. A. Leech, J. W., and Morins, L., PETROS 3: A Finite-Difference Method and Program for the Calculation of Large Elastic-Plastic Dynamically-Induced Deformations of Multi-Layer, Variable-Thickness Shells, BRL CR 60 (MIT-ASRL TR 152-2) November 1971.

8. Ross, C. A., and Milton, J. E., Study of Dynamic Response of Shell Structures to Blast Loads, AFATL-TR-75-117, USAF Armament Laboratory, Eglin AFB FL, September 1975.

9. Goodman, H. J., Compiled Free-Air Blast Data on Bare Spherical Pentolite, BRL Department No. 1092, Ballistic Research Laboratory Aberdeen Proving Ground MD, February 1960.

10. Zumwalt, G. W., and Naik, S. N., Computer Program for a Blast Wave Passing a Cylinder," Department of Aeronautical Engineering, Wichita State University, Wichita Kansas, July 30, 1975.

11. Reynolds, T. E., "Inelastic Lobar Buckling of Cylindrical Shells Under External Hydrostatic Pressure," David Taylor Modal Basin Department, 1392, August 1960.

12. Almroth, B. O., "Buckling of a Cylindrical Shell Subjected to Nonuniform External Pressure," Journal of Applied Mechanics, Volume 29, Ser. E, No. 4, December 1962, pp. 675-682.

INITIAL DISTRIBUTION

HQ USAF/RDQRM	1	NASA Langley Rsch Cntr	1
HQ USAF/SAMI	1	TAC/INAT	1
DEFENSE INTEL AGCY	1		
HQ USAFE/DOQ	1		
HQ PACAF/DOOFQ	3		
HQ AFSC/SDZA	1		
HQ TAC/XPSY	1		
HQ TAC/DRA	1		
HQ TAC/DRFA	1		
AFFDL/FES	1		
ASD/ENFEA	1		
ASD/ENESH	1		
AUL/LSE 71-249	1		
USAFTFWC/OA	1		
USAFTFWC/TE	1		
HQ SAC/DOOB	1		
HQ SAC/NRI/Stinfo Lib	1		
NAV WPNS CNTR/Code 318	2		
NAV WPNS CTR/Code 317	2		
AFSC LIASON OFFICE/Code 03A4	2		
OO/ALC/MMWMP	2		
AFIS/INT	1		
DDC-DDA	2		
AFATL/DLODL	2		
AFATL/DL	1		
AFATL/DLJ	1		
AFATL/DLD	1		
AFATL/DLY	1		
ADTC/XR	1		
ADTC/XRS	1		
ADTC/INH	1		
SACPO	1		
TAWC/OA	1		
ASD/ENFEA	1		
US Army Tradoc Sys Ana Act	1		
ASD/XRP	1		
COMIPAC/I-232	1		
HQ AFSC/XRPA	1		
HQ USAF/AFRD	1		
SAF/SAFRD	1		
ASD/XRO	2		
AMSAA/DRXSY-J	1		

(The reverse of this page is blank)